Theoretical Study of Bonding, Structure, and Vibrational Spectra of the $[Fe_2(CO)_8]^{2-}$ Anion and Its Derivatives†

Gabriel Aullón* and Santiago Alvarez

Departament de Química Inorgànica and Centre Especial de Recerca en Química Teòrica (CeRQT), Universitat de Barcelona, Diagonal 647, 08028 Barcelona, Spain

Received June 26, 2000

A theoretical study of the structural versatility of the di-iron carbonylate, $[Fe_2(CO)_8]^{2-}$, and of its adducts with electrophiles is presented. The geometries of three energy minima and four transition states of $[Fe_2(CO)_8]^{2-}$ have been characterized, and the relative energies of several alternative structures have been evaluated. The calculated vibrational spectra in the Fe−Fe and the C≡O stretching regions are discussed for the three isomers, and a good correlation between the Fe−Fe stretching force constant and the Fe−Fe bond distance is found for both theoretical and experimental data. The effect of the orientation of the terminal ligands on the Fe−Fe bond and the rearrangement of such ligands by the formation of adducts with electrophiles are also addressed.

Downloaded by CARLI CONSORTIUM on June 29, 2009
Published on February 6, 2001 on http://pubs.acs.org | doi: 10.1021/om000548e

The carbonylate anion $[Fe_2(CO)_8]^{2-}$ and its isoelectronic Ru and Os analogues are interesting molecules from the structural point of view. They all present metal−metal bonding, but at least three different structures are found that differ in the local coordination around each metal atom, square pyramidal or trigonal bipyramidal[1,2] Furthermore, the carbonylate anion $[Fe_2(CO)_8]^{2-}$ can form adducts with Lewis acids in either terminal or bridging positions. For instance, methylene-bridged complexes can be obtained by reacting this anion with CH_2X_2 species.[3] On the other hand, $[Fe_2(CO)_8]^{2-}$ is a versatile building block for the construction of a variety of clusters[4] by reaction with metal ions.

Analyzing the structures of some carbonyl compounds with Fe−Fe bonds,[5,6] we have observed that the Fe−Fe and Fe−electrophile distances span wide ranges, depending on the orientation of the carbonyl ligands. We therefore decided to undertake a theoretical study of the structure of the $Fe_2(CO)_8$ fragment, both in the isolated dianion $[Fe_2(CO)_8]^{2-}$ and in the adducts that it forms with electrophiles, in an attempt to rationalize the shapes in which it appears in different molecules and the influence of the ligands' orientation on the Fe−Fe and Fe−electrophile bonds. Thus, we report in this paper a systematic density functional (DFT) study of the $[Fe_2(CO)_8]^{2-}$ anion and of its adducts $[Fe_2(\mu\text{-}CH_2)(CO)_8]$ and $[Fe_2Me_2(CO)_8]$. Also the vibrational spectra have been calculated, to provide some hints for the characterization of the different tautomers for which no X-ray structural data are available, focusing mostly on the infrared-active CO stretching modes and the Raman-active Fe−Fe stretching vibrations.

Table 1. Calculated Relative Energies (kcal/mol) and Fe−Fe Bond Distances (Å) for Different Geometries of $[Fe_2(CO)_8]^{2-}$

structure		symmetry	energy	Fe−Fe
1a	**aT−aT**	D_{3d}	1.1[a]	2.852
1b	**eS−eS**	C_{2v}	2.8[a]	2.629
1c	**eT−eT**	D_{2d}	0.0[a]	2.734
1d	**eT−eT**	D_{2h}	16.7	3.045
1e	**aS−aS**	D_{4h}	35.7	2.729
1f	**aS−aS**	D_{4d}	34.1	2.700
1g	**aT−aT**	D_{3h}	10.7	3.115
1h	**eT−eS**	C_s	2.2[b]	2.771
1j	**eT−aT**	C_s	7.1[b]	2.901
1k	**aT−aS**	C_s	17.4[b]	2.808
TS1			3.4	2.659
TS2			4.6	2.832

[a] Energy minimum. [b]Nonstationary points of the potential energy surface.

Relative Stabilities of the Structures of $[Fe_2(CO)_8]^{2-}$. We can imagine the binuclear compound $[(OC)_4Fe-Fe(CO)_4]^{2-}$ to be formed by fusing together two $Fe(CO)_4^-$ fragments through Fe−Fe bonding, in such a way that the coordination environment of each Fe atom can be deduced from that in the parent complex $[Fe(CO)_5]$ by replacing an Fe−C by an Fe−Fe bond. Thus, a variety of geometries for the dianion can be envisaged by combining square pyramidal (SP) and trigonal bipyramidal (TBP) geometries of the two moieties and axial or equatorial positions of the Fe−Fe bond, as schematically represented in **1**. To help identify the different geometries, we have chosen to label the local coordination polyhedra of each Fe atom with a capital letter (**T** for a trigonal bipyramid, **S** for a square pyramid) and the connectivity of the two polyhedra by a small case letter (**e** for an equatorial, **a** for an axial

† Dedicated to Prof. Rafael Usón on the occasion of his 75th birthday.

(1) Shriver, D. F.; Whitmire, K. H. In *Comprehensive Organometallic Chemistry*; Wilkinson, G., Stone, F. G. A., Abel, E. W., Eds.; Pergamon: New York, 1982; Vol. 4, p 259.
(2) Bruce, M. I. In *Comprehensive Organometallic Chemistry II*; Abel, E. W., Stone, F. G. A., Wilkinson, G., Shriver, D. F., Bruce, M. I., Eds.; Pergamon Press: New York, 1995; Vol. 7; p 300.
(3) Fagan, P. J. In *Comprehensive Organometallic Chemistry II*; Abel, E. W., Stone, F. G. A., Wilkinson, G., Shriver, D. F., Bruce, M. I., Eds.; Pergamon Press: New York, 1995; Vol. 7, p 237.
(4) Ferrer, M.; Reina, R.; Rossell, O.; Seco, M. *Coord. Chem. Rev.* **1999**, *193−195*, 619.
(5) Rossell, O.; Seco, M.; Segalés, G.; Alvarez, S.; Pellinghelli, M. A.; Tiripicchio, A.; de Montauzon, D. *Organometallics* **1997**, *16*, 236.
(6) Alvarez, S.; Aullón, G. In *Metal Clusters in Chemistry*; Braunstein, P., Oro, L. A., Raithby, P. R., Eds.; Wiley-VCH: Weinheim, 1999; Vol. 1, p 30.

10.1021/om000548e CCC: $20.00 © 2001 American Chemical Society
Publication on Web 02/06/2001

Scheme 1

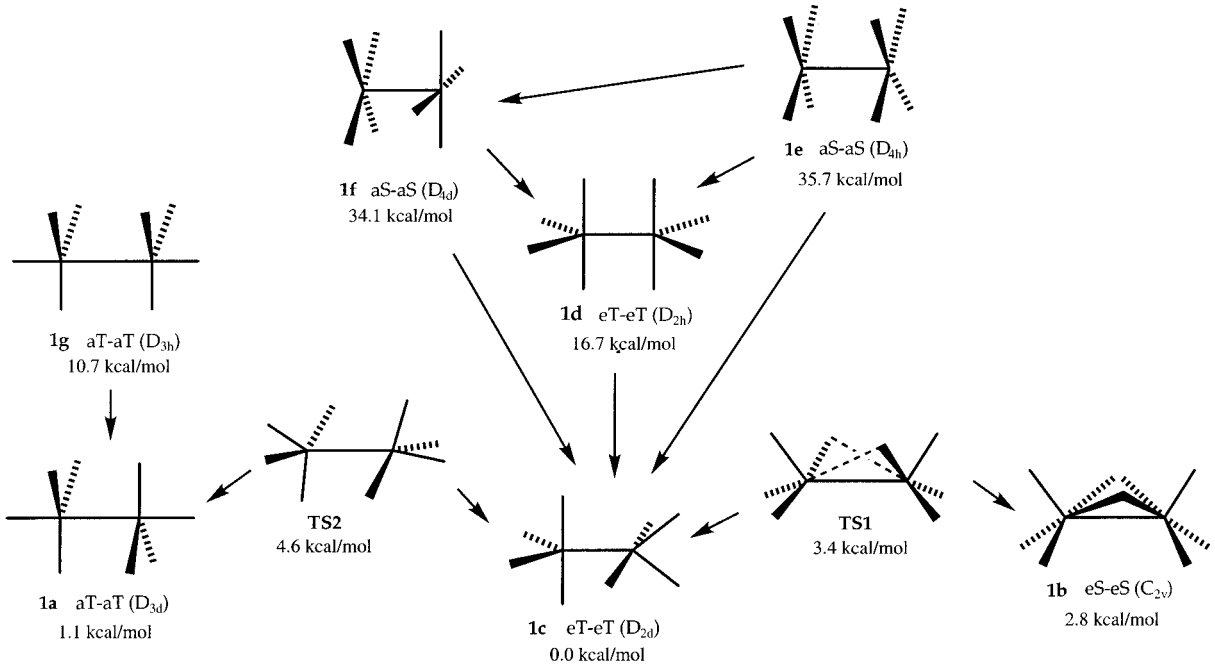

position of the Fe−Fe bond within each polyhedron). In some cases we have investigated two alternative structures with the same polyhedra and connectivity that are related by rotation of the two $Fe(CO)_4$ fragments around the Fe−Fe bond (i.e., structures **1a** and **1g**, **1c** and **1d**, and **1e** and **1f**).

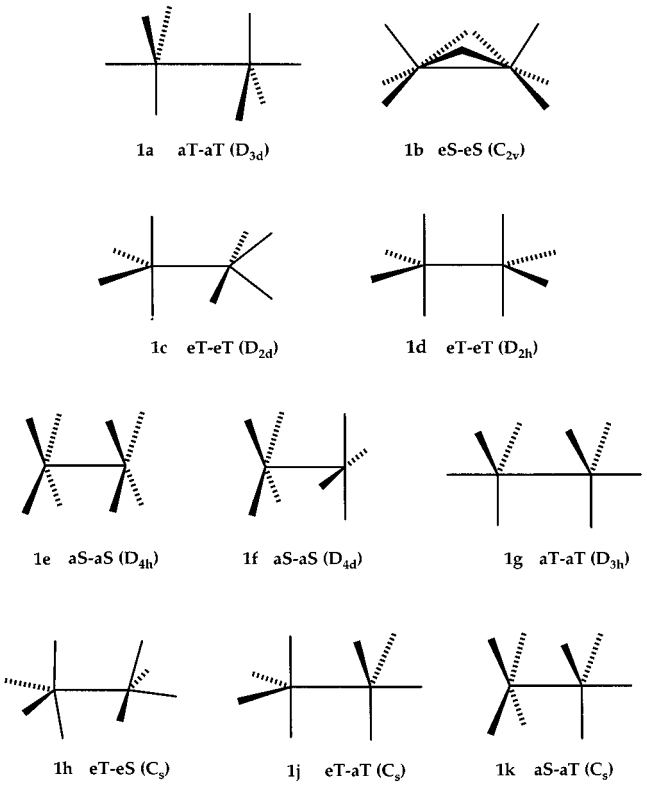

The calculated energies for structures **1a**−**1k** are summarized in Table 1. Among these structures, only **1a**−**1c** correspond to minima in the potential energy surface, according to the analysis of the calculated vibrational frequencies (see below), and these are all very similar in energy. In addition, two transition states could be located, **TS1** and **TS2**, corresponding to the **1b**−**1c** and **1a**−**1c** interconversions, respectively (Scheme 1). No transition state could be located between **1a** and **1b**, indicating that their interconversion must proceed through **1c**. Given the small energy involved along the **1a**−**1c**−**1b** pathway and the anionic nature of the species under study, we can anticipate that geometries along such path should be expected due to modifications of the potential energy surface associated with ionic interactions or ligand substitution. All the salts of [$Fe_2(CO)_8$]$^{2-}$ that have been structurally characterized,[7−13] as well as other isoelectronic metal carbonylates, present the **aT**−**aT** structure **1a** in the solid state (Table 2). The existence of isomers of [$Fe_2(CO)_8$]$^{2-}$

Table 2. Geometrical Data for Compounds of General Formulas $A_2[M_2(CO)_8]$ (M = Fe, Os) Isoelectronic with [$Fe_2(CO)_8$]$^{2-}$ with Structure 1a[a]

compd	M−M (Å)	α (deg)	refcode	ref
[Fe(im)$_6$][$Fe_2(CO)_8$]	2.770	83.7	MIMFEA	7
(lut)$_2$[$Fe_2(CO)_8$]	2.779	83.9	ZIQNIW	8
({PPh_3}$_2$N)$_2$[$Fe_2(CO)_8$]	2.787	83.3	TPIFEC	9
({PPh_3}$_2$CH)$_2$[$Fe_2(CO)_8$]	2.786	84.0	GIYLEF	10
(PPh_4)$_2$[$Fe_2(CO)_8$]	2.793	83.9	TABMUE	11
[Na(py)$_4$]$_2$[$Fe_2(CO)_8$]	2.815	83.3	PAGVIC	12
(Et_4N)$_2$[$Fe_2(CO)_8$]	2.844	85.3	YACLET	13
(PPh_4)$_2$[$Os_2(CO)_8$]	2.990	83.2	DELHOR	17
	2.997	83.7		

[a] Abbreviations: im = *N*-methylimidazole; lut = *N*-methyllutidinium; py = pyridine.

(7) Seel, F.; Lehnert, R.; Bill, E.; Trautwein, A. *Z. Naturforsch., Teil B* **1980**, *35*, 631.
(8) Bockman, T. M.; Cho, H.-C.; Kochi, J. K. *Organometallics* **1995**, *14*, 5221.
(9) Chin, H. B.; Smith, M. B.; Wilson, R. D.; Bau, R. *J. Am. Chem. Soc.* **1974**, *96*, 5285.
(10) Petz, W.; Weller, F. *Z. Kristallogr.* **1997**, *212*, 157.
(11) Bhattacharyya, N.; Coffy, T. J.; Quintana, W.; Salupo, T. A.; Bricker, J. C.; Shay, T. B.; Payne, M.; Shore, S. G. *Organometallics* **1990**, *9*, 2368.
(12) Deng, H.; Shore, S. G. *Inorg. Chem.* **1992**, *31*, 2289.
(13) Cassidy, J. M.; Whitmire, K. H.; Long, G. J. *J. Organomet. Chem.* **1992**, *427*, 355.

Downloaded by CARLI CONSORTIUM on June 29, 2009
Published on February 6, 2001 on http://pubs.acs.org | doi: 10.1021/om000548e

Table 3. Experimental Structural Data for 1b Compounds Isoelectronic with $[Fe_2(CO)_8]^{2-}$ (see 2a for definition of θ and β)

compound	M−M (Å)	θ (deg)	β (deg)	refcode	ref
$[Fe_2(\mu\text{-}CNEt_2)_2(CO)_6]$	2.480	207.7	102.3	EIMFEC10	20, 21
$(\{PPh_3\}_2N)[Fe_2(\mu\text{-}SO_2)_2(CO)_6]$	2.636	205.9	100.9	HIWKIH	22
$[Co_2(\mu\text{-}CO)_2(CO)_6]$	2.536	193.6	100.1	FOHDEL04	18, 19
	2.539	192.6	100.0		
$[Co_2(\mu\text{-}CNC_6H_3Me_2)_2(CNC_6H_3Me_2)_6]$	2.469	198.5	99.9	LIDVOJ	23
$[Co_2(\mu\text{-}CN^tBu)_2(CN^tBu)_6]$	2.457	203.1	101.1	TBICCO10	24

other than **1a** in solution has been detected by Raman spectroscopy,[14] in agreement with the small energy differences predicted by our calculations. A similar behavior has long been known for the isoelectronic $[Co_2(CO)_8]$, for which the transformation between bridged and unbridged forms was early detected by infrared spectroscopy.[15,16]

The **eS**−**eS** structure (**1b**) was proposed for a second isomer of $[Fe_2(CO)_8]^{2-}$, by analogy with that found in the solid state for the isoelectronic compound $[Co_2(CO)_8]$.[18,19] Although no crystal structure of type **1b** has been reported for $[Fe_2(CO)_8]^{2-}$ so far, a few isoelectronic compounds have been found with such structure (Table 3). The square pyramidal nature of the FeC_5 cores can be seen in the average of the $C_{ax}-Fe-C_{eq}$ bond angles (β), which is close to 100° both in the calculated and in the related experimental structures. Such structural unit is also present in the adducts formed upon reacting $[Fe_2(CO)_8]^{2-}$ with some electrophiles (see below).

Other geometries obtained by fusing two $Fe(CO)_4$ polyhedra (isomers **1d**−**1g**) are relatively high in energy and present imaginary frequencies that relate them with other structures, as indicated by the arrows in Scheme 1. Therefore, we do not expect these geometries to show up in crystal structures, but some of them could be relevant for dynamic processes at room temperature. The **1g** and **1d** forms correspond to the transition states for the rotation around the Fe−Fe bond of **1a** and **1c**, respectively, with calculated activation energies of 9.6 and 16.7 kcal/mol, respectively.

The structure based on two square pyramids forming an Fe−Fe bond through the axial positions (**aS**−**aS**), in either its eclipsed **1e** or staggered **1f** conformations, is seen to be more than 34 kcal/mol above the minimum **1c**. The three imaginary modes of **1e** reflect the greater stability of the trigonal bipyramidal local geometry compared to the square pyramid and three different paths for conversion to the stable isomer **1c**: (i) directly through a B_{2u} mode, (ii) through a **1f** transition state obtained by rotation around the Fe−Fe bond (A_{1u} mode), or (iii) through the **1d** form (B_{1g} mode). As expected from the high energy calculated for these two structures (Table 1), no compounds of this structure isoelectronic with $[Fe_2(CO)_8]^{2-}$ have been found in a structural database search. However, $M_2(CO)_8$ fragments (M = Ru, Os) with **1e** or **1f** structures appear in adducts with two electrophiles attached to the empty axial coordination positions (see discussion on adducts below).

Structures **1h**, **1j**, and **1k** do not correspond to stationary points in the potential energy surface. The irregular structure **1h** (only 2.2 kcal/mol above **1c** in our calculations) is unknown for the octacarbonyldiferrate(2−) anion, but ruthenium carbonylate complexes of the type $[MRu(CO)_8]^{2-}$, with M = Ru[17] or Fe,[11] present such structure in the solid state. That structure can be derived by distorting the more symmetric isomer **1c** via a concerted motion of the carbonyl ligands of one $Fe(CO)_4$ fragment, monitored by the angle χ (the angle between the metal−metal bond and the bisector of the two equatorial M−C bonds, **2b**). This parameter is 0° for the symmetric **1c** geometry and increases along the distortion path. When this distortion is taken to $\chi \approx 20°$, the angles around one Fe atom correspond to a square pyramid,[25] resulting in the **1h** geometry that can be described as **eT**−**eS**. The potential energy curve is shallow, and **1h** is calculated to be only 2.2 kcal/mol higher than **1c**. The agreement between the calculated (Fe_2 anion) and experimental (Ru_2 and FeRu anions) angular parameters is good, except for those angles involving semibridging carbonyl groups, given the differences in M−M distances between the calculated (Fe−Fe) and experimental (Fe−Ru or Ru−Ru) complexes. Another interesting geometry corresponds to $\chi \approx 48°$. In this case, a structure based on two trigonal bipyramidal Fe atoms (**1j**) results. Such structure, which was proposed for the third isomer of $[Co_2(CO)_8]$,[26] appears in our calculations 7.1 kcal/mol higher than that of **1c** for $[Fe_2(CO)_8]^{2-}$.

The mixed metal compound $[FeCo(CO)_8]^-$ presents a structure similar to **1h** with $\chi \approx 9°$ and an asymmetrically bridging carbonyl between the $Fe(CO)_4$ and $Co(CO)_3$ fragments.[9] It is interesting to notice that this structure is intermediate between those found in the solid state for $[Fe_2(CO)_8]^{2-}$ (**1a**) and $[Co_2(CO)_8]$ (**1b**).

Molecular Structure and Fe−Fe Bonding. In this section we present the structural data calculated for the different structures of $[Fe_2(CO)_8]^{2-}$ (Table 4) and analyze the effect of the ligand orientation on the Fe−Fe bond. The first relevant observation that can be made is that the Fe−Fe bond length in the three stable structures (**1a**−**1c**) is strongly affected by the molecular geometry, despite the small energy differences among

Downloaded by CARLI CONSORTIUM on June 29, 2009
Published on February 6, 2001 on http://pubs.acs.org | doi: 10.1021/om000548e

(14) Onaka, S.; Shriver, D. F. *Inorg. Chem.* **1976**, *15*, 915.
(15) Noack, K. *Spectrochim. Acta* **1963**, *19*, 1925.
(16) Bor, G. *Spectrochim. Acta* **1963**, *19*, 2065.
(17) Hsu, L.-Y.; Bhattacharyya, N.; Shore, S. G. *Organometallics* **1985**, *4*, 1483.
(18) Sumner, G. G.; Klug, H. P.; Alexander, L. E. *Acta Crystallogr.* **1964**, *17*, 732.
(19) Leung, P.; Coppens, P. *Acta Crystallogr., Sect. B* **1983**, *39*, 535.
(20) Cash, G. G.; Pettersen, R. C.; King, R. B. *J. Chem. Soc., Chem. Commun.* **1977**, 30.
(21) Pettersen, R. C.; Cash, G. G. *Acta Crystallogr., Sect. B* **1977**, *33*, 2331.
(22) Eveland, R. W.; Raymond, C. C.; Albrecht-Schmitt, T. E.; Shriver, D. F. *Inorg. Chem.* **1999**, *38*, 1282.
(23) Leach, P. A.; Geib, S. J.; Corella, J. A., II; Warnock, G. F.; Cooper, N. J. *J. Am. Chem. Soc.* **1994**, *116*, 8566.
(24) Carroll, W. E.; Green, M.; Galas, A. M. R.; Murray, M.; Turney, T. W.; Welch, A. J.; Wodward, P. *J. Chem. Soc., Dalton Trans.* **1980**, 80.
(25) Muetterties, E. L.; Guggenberger, L. J. *J. Am. Chem. Soc.* **1974**, *96*, 1748.
(26) Lichtenberger, D. L.; Brown, T. L. *Inorg. Chem.* **1978**, *17*, 1381.

Table 4. Structural Parameters for the Optimized Structures of $[Fe_2(CO)_8]^{2-}$

parameter[a]	**1a** (D_{3d})	**1b** (C_{2v})	**1c** (D_{2d})	**1d** (D_{2h})	**1e** (D_{4h})	**1f** (D_{4d})	**1g** (D_{3h})
Fe−Fe	2.852	2.629	2.734	3.045	2.729	2.700	3.115
Fe−C_{eq}	1.773	1.769	1.744	1.742	1.775	1.775	1.775
Fe−C_a	1.735	1.741	1.781	1.787			1.729
Fe−C_b	1.981						
Fe−Fe−C_{eq}	83.8	111.4	125.0	121.1	98.0	97.7	86.1
Fe−Fe−C_a		123.8	75.9	83.9			
C_{eq}−Fe−C_{eq}	118.9				88.9	89.0	119.6
C_a−Fe−C_{eq}		106.2	98.1	93.2			
C_a−Fe−C_b		95.1					
C_b−Fe−C_b		83.9					
Fe−C_b−Fe		83.1					
θ		194.4					

[a] Notation: a = axial (or apical), b = bridging, eq = equatorial (or basal).

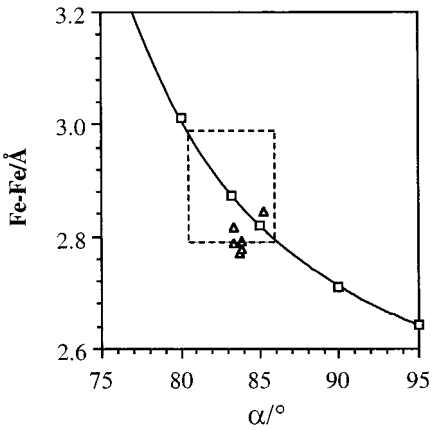

Figure 1. Calculated Fe−Fe bond distances as a function of the pyramidality angle α in $[Fe_2(CO)_8]^{2-}$ (squares) with structure **1a**. The inset represents the geometries that fall within 2 kcal/mol from the calculated minimum. Experimental data for different salts of the dianion are also represented (triangles).

them. The optimized Fe−Fe bond distance in **1a** is 2.852 Å, close to the experimental values (2.77−2.84 Å, Table 2). The calculated degree of pyramidalization around the Fe atoms, indicated by the M−M−C_{eq} bond angle, α, is 83.8°, in excellent agreement with the experimental data. Simple rotation of the two moieties around the Fe−Fe bond to give the eclipsed structure **1g** increases the metal−metal distance to a long 3.115 Å and the pyramidality angle to 86.1° due to ligand···ligand repulsions. We have analyzed the relationship between the metal−metal distance and the pyramidality (α) in $[Fe_2(CO)_8]^{2-}$ with structure **1a**, and the result is shown in Figure 1. One can see there that an increase in the degree of pyramidality around the Fe atoms results in a shorter calculated Fe−Fe bond length. This trend is not apparent in the experimental data of the different salts of the carbonylate dianion (Table 2) because all of them present very similar bond angles. It must be noticed, however, that changes in the Fe−Fe distance of around 0.1 Å (corresponding to a angles between 80° and 86°) destabilize the molecule by only 2 kcal/mol, comparable to the energy of interaction with the counterions. Hence, one can expect new salts of this dianion to present significantly different Fe−Fe distances.

For the subsequent discussion we wish to consider the orientation of the terminal CO ligands in the CO-bridged isomer **1b**. Hence, we define a vector from the Fe atom to the centroid of the triangle formed by the three terminal carbonyls and take the angle that such vector forms with the Fe−Fe bond (θ in **2a**) as a measure of the orientation of the $Fe(CO)_3$ pyramid. The calculated value of θ in **1b** is 194.4°, well within the range exhibited by related experimental structures (Table 3), in which the $Fe(CO)_3$ pyramid is bent away from the bridging carbonyls toward the empty coordination site of the Fe atoms (θ > 180°), as seen also by the large C_{ax}−Fe−C_{eq} bond angles (106°) compared to the C_{ax}−Fe−C_b ones (95°). We observe, though, that both the metal−metal distances and the orientation angles show a wide dispersion. Therefore, we decided to study the effect of the orientation of the $Fe(CO)_3$ pyramids on the total energy and on the Fe−Fe bond distance (Figure 2). There, it is clearly seen that the Fe−Fe distance decreases as θ increases. We compare this theoretical trend with experimental data for isoelectronic compounds (Table 3), including the Co analogues, for which a dependence of the metal−metal distance on θ is also found (Figure 2), even if the calculated distances are slightly larger than the corresponding experimental ones.

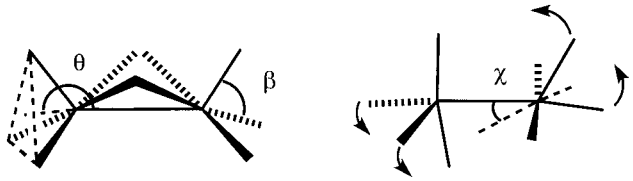

2a eS-eS **2b eT-eS**

In isomer **1c**, the optimized Fe−Fe bond distance (2.734 Å) is significantly shorter than in **1a** (2.852 Å). The Fe−Fe−C angles for the carbonyl ligands in axial and equatorial positions (125.0° and 75.9°, respectively) are consistent with the description of the Fe coordination sphere as a trigonal bipyramid, but may also be indicative of a semibridging carbonyl, with a nonbonded Fe···C distance of 2.874 Å. We are not aware of the existence of structurally charcterized carbonyl complexes having the D_{2d} geometry (**1c**), although some experimental data may be consistent with such symmetry. Poor crystals of the isoelectronic $[Rh_2(PF_3)_8]$ having Rh−Rh ≈ 2.88 Å were obtained by Bennett et al.,[27] and the presence of two ligand signals in a 1:1 ratio in its ^{19}F and ^{31}P NMR spectra suggests the **1c** structure.

The optimized bond distances in the **1h** geometry of $[Fe_2(CO)_8]^{2-}$ are very close to those of the undistorted

(27) Bennett, M. A.; Johnson, R. N.; Turney, T. W. *Inorg. Chem.* **1976**, *15*, 2938.

Downloaded by CARLI CONSORTIUM on June 29, 2009
Published on February 6, 2001 on http://pubs.acs.org | doi: 10.1021/om000548e

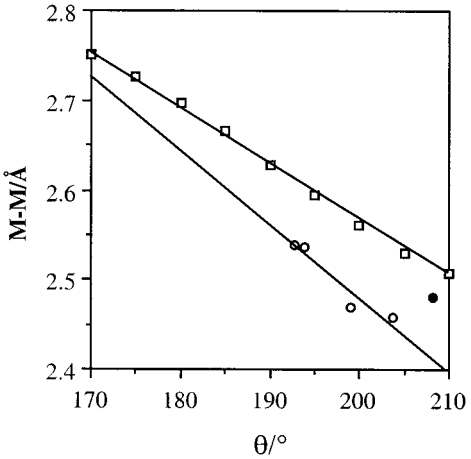

Figure 2. Calculated Fe−Fe bond distances as a function of the orientation of the terminal carbonyls (θ defined in **2a**) in the C_{2v} structure of $[Fe_2(CO)_8]^{2-}$ (**1b**). Experimental data for isoelectronic iron (black circles) and cobalt complexes (white circles) are shown for comparison.

Table 5. Calculated and Experimental Raman[14] Fe−Fe Stretching Wavenumbers ($\bar{\nu}_{FeFe}$, cm^{-1}), Together with Calculated Fe−Fe Distance (Å) for the Studied Isomers of $[Fe_2(CO)_8]^{2-}$

structure	Fe−Fe	$\bar{\nu}_{FeFe}$ calcd.	$\bar{\nu}_{FeFe}$ expt
1b (C_{2v})	2.629	225	222[a]
1c (D_{2d})	2.734	177	
1a (D_{3d})	2.852	158	
			167−168[a]
			161−178[b]
1d (D_{2h})	3.045	118	
1e (D_{4h})	2.729	182	
1f (D_{4d})	2.700	189	
1g (D_{3h})	3.115	98	
TS1	2.832	159	
TS2	2.659	212	

[a] DMF solution. [b] Solid state.

structure **1c**. In either eclipsed (**1e**) or staggered (**1f**) conformation the optimized structures present short Fe−Fe distances of around ∼2.7 Å and a similar degree of pyramidalization (∼98°).

In summary, comparison of the different calculated structures (Table 4) indicates that shorter Fe−Fe bond distances appear when the two Fe atoms are in a square pyramidal arrangement. For the trigonal bipyramidal coordination, the staggered rotamers present shorter distances than the eclipsed ones, a fact that can be attributed to the steric interligand repulsion in the eclipsed conformation. Other things being equal, it is seen that equatorial Fe−Fe bonds are shorter than axial ones. Given the differences in coordination spheres and connectivity between the two monomeric units in the studied structures, it is not surprising that no correlation is found between the optimized Fe−Fe distance and the calculated energy for each isomeric form.

Vibrational Spectra. The theoretical study of the vibrational spectra of carbonyl complexes is of interest because they usually are useful as a structural diagnostic tool for the solid-state compounds and for detecting isomerization reactions in solution. Hence, we report in this section the calculated spectra for all those structures of $[Fe_2(CO)_8]^{2-}$ that have been found to be stationary points in the potential energy surface. We will focus only on the two most relevant regions of the vibrational spectra, notably the low-frequency metal−metal stretching and the high-frequency C−O stretching modes.

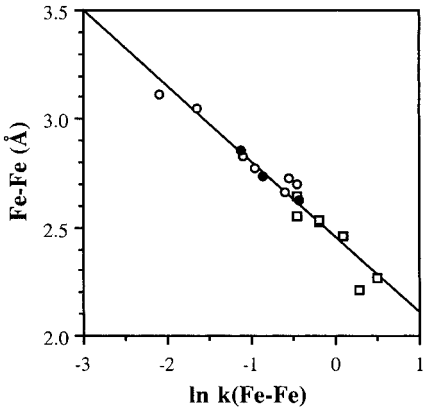

Figure 3. Relationship between the Fe−Fe bond distance and stretching force constant. The straight line represents the least-squares fitting of both experimental (squares) and calculated data (solid circles for minima, empty circles for other structures and transition states), given by eq 1.

The calculated Fe−Fe stretching frequencies for the different tautomers are shown in Table 5. A clear correlation is found between those frequencies and the optimized Fe−Fe distance for each isomer. Moreover, the calculated data nicely extend the Herschbach−Laurie logarithmic relationship between the stretching force constant (k_{FeFe}) and the Fe−Fe distance reported by Harvey[28] based on experimental data (Figure 3). It is noteworthy that the least-squares parameters for the extended correlation (eq 1) are very close to those reported by Harvey.

$$Fe-Fe = 2.452-0.348 \ln(k_{FeFe}) \qquad (1)$$

Bimetallic carbonyl complexes of first-row transition metals with a metal−metal bond present a Raman band in the 100−200 cm^{-1} range, which appears shifted above 200 cm^{-1} when the metal−metal bond is bridged by carbonyl ligands.[29] Consistent with this principle, the highest calculated value of $\bar{\nu}_{FeFe}$ corresponds to the carbonyl-bridged complex **1b**. The theoretical value (225 cm^{-1}) is in excellent agreement with that observed for several salts of $[Fe_2(CO)_8]^{2-}$ (222 cm^{-1}).[14] The band observed for $[Fe_2(CO)_8]^{2-}$ in solution at 168 cm^{-1} could be assigned to either the **1a** or the **1c** structure, according to our results. The fact that the bands observed in the solid state appear scattered through a range of 17 cm^{-1} can be attributed to the different Fe−Fe distances observed (Table 2), according to the bond length−force constant correlation (Figure 3).

The second region of the vibrational spectra that we analyze here corresponds to the carbonyl stretching modes, that can be clearly seen in the infrared without interference from other modes. The calculated bands for the different stationary points of $[Fe_2(CO)_8]^{2-}$ are presented in Table 6. The characteristic shift of the bridging carbonyl bands to lower wavenumbers[29] is clearly observed for the **1b** structure, at 1685 and 1693 cm^{-1}. It must be stressed that such vibrations present strong

(28) Harvey, P. D. *Coord. Chem. Rev.* **1996**, *153*, 175.
(29) Housecroft, C. E. *Metal−Metal Bonded Carbonyl Dimers and Clusters*; Oxford University Press: Oxford, 1996; Vol. 44.

Downloaded by CARLI CONSORTIUM on June 29, 2009
Published on February 6, 2001 on http://pubs.acs.org | doi: 10.1021/om000548e

Table 6. Calculated Carbonyl Stretching Frequencies (in cm^{-1}) and Infrared Intensities (in parentheses, $km \cdot mol^{-1}$) for the Three Geometries of $[Fe_2(CO)_8]^{2-}$ Corresponding to Minima in the Potential Energy Surface.

range	**1a** (D_{3d})	**1b** (C_{2v})	**1c** (D_{2d})
1900−1950	A_{1g} 1932	A_1 1923 (23)	A_1 1931
1820−1860	A_{2u} 1846 (2651)	B_1 1857 (2427)	B_2 1842 (2304)
	E_u 1830 (2659)	B_2 1827 (2240)	E 1830 (2754)
		A_1 1820 (2666)	
1750−1820	A_{1g} 1815	A_2 1814	B_2 1819 (430)
	E_g 1803	B_1 1809 (45)	A_1 1811
	A_{2u} 1796 (519)		E 1792 (78)
1650−1700		A_1 1693 (375)	
		B_2 1685 (916)	

mixing with Fe−C stretching modes. For that structure, three additional infrared bands are expected between 1800 and 1900 cm^{-1}. In contrast, only two intense bands between 1830 and 1850 cm^{-1} are expected in the spectra of both the **1c** and **1a** isomers. Most modes are combinations of axial and equatorial CO vibrations, except for the E_u and E_g modes of the **1a** isomer, and B_2 and A_2 of the **1b** structure, which can be clearly assigned to equatorial CO stretchings.

In the **1a** structure found for the salts of $[Fe_2(CO)_8]^{2-}$, three infrared-active ν(CO) bands are predicted by our calculations at 1846 (A_{2u}), 1830 (E_u), and 1796 cm^{-1} (A_{2u}). The former is in excellent agreement with the experimental values of 1844−1855 cm^{-1} reported in the solid state (KBr or Nujol mull; spectral data and references provided as Supporting Information). The E_u band is observed at 1829−1833 cm^{-1} in the solid state, but shifted to 1840 cm^{-1} in acetonitrile solution,[8] probably indicating the existence of an isomerization process predicted by the low energy barriers between **1a**−**1c**. The third band of A_{2u} symmetry, predicted at 1796 cm^{-1} with low intensity, is not detected experimentally. Some authors have assigned bands at 1908−1927 cm^{-1} to this mode, but our results suggest that these might correspond to the infrared-forbidden A_{1g} mode (calculated at 1932 cm^{-1}), probably due to symmetry loss in condensed media.

Bonding Ability of the $[Fe_2(CO)_8]^{2-}$ Anion. In this section we analyze the influence of the conformation of this anion on its bonding ability toward electrophiles E. In principle, one should expect **1b**, **1c**, and **1d** to have the lone pairs centered at the Fe atoms oriented toward the bridging zone, thus giving the corresponding adducts **3b** and **3c**, whereas form **1a** or **1g** has the lone pairs directed between two equatorial ligands and should give adducts of type **3a**.[30] Finally, forms **1e** and **1f** have their lone pairs pointing to the vacant axial positions and can give adducts **3e**. A structural database search, carried out with the help of the Cambridge Structural Database,[31] allowed us to identify the structures of adducts of group 8 anions $[M_2(CO)_8]^{2-}$ with a variety of electrophiles, including ML_n fragments that give place to trinuclear clusters. The results (provided as Supporting Information) can be summarized as follows: (i) Adducts of the type **3c** are relatively common and present a great variety of electrophiles. (ii) Some electrophiles, such as R_2C or d^{10}-ML, are bound in either the **3b** or **3c** forms. (iii) The structural preferences are different for Fe than for the heavier elements. For instance, Fe gives only **3b** derivatives with d^8-ML_4 fragments, whereas Ru and Os give mostly the **3c** isomer. (iv) The **1d** anion may add one or two electrophiles, forming adducts **3c** or **3c′**, whereas **1e** or **1f** always adds two electrophiles as in **3e**.

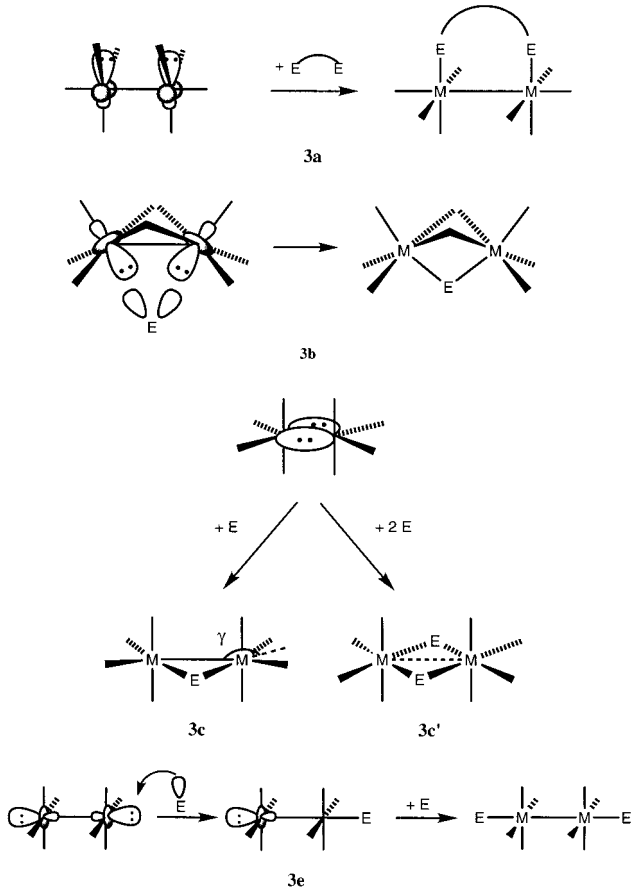

Let us start by analyzing the bonding of an electrophile in the **3b** structure of $[Fe_2(CO)_6(\mu\text{-}CO)_2(\mu\text{-}E)]$. Since the parent **1b** dianion is a minimum only about 3 kcal/mol above its most stable form **1c**, it is not strange that such adducts are very easily formed (Supporting Information). An important effect of the attachment of an electrophile in the bridging position in these species is the reorientation of the terminal carbonyl ligands. Taking the methylene as electrophile, $[Fe_2(CO)_6(\mu\text{-}CO)_2(\mu\text{-}CH_2)]$, the value of θ (defined in **2a**) at the optimized structure is 182°, to be compared with the theoretical value for the parent carbonylate **1b** of 194°. Hence, the anion must undergo a rearrangement to form the adduct, although the cost of such deformation has been evaluated to be of only 2 kcal/mol within the range 182° $< \theta <$ 204°. Another structural change that is predicted upon bonding of the electrophile is a significant shortening of the metal−metal bond distance (2.505 Å in the adduct compared to 2.629 Å in the dianion), despite the effect that a decreased value of θ is expected to have on that distance on the parent dianion (Figure 2). In fact, it can be seen that the effect of the orientation of the terminal ligands on the Fe−Fe distance is drastically reduced upon incorporation of the electrophile (Figure

(30) Alvarez, S.; Rossell, O.; Seco, M.; Valls, J.; Pellinghelli, M. A.; Tiripicchio, A. *Organometallics* **1991**, *10*, 2309.
(31) Allen, F. H.; Kennard, O. *Chem. Des. Autom. News* **1993**, *8*, 31.

Downloaded by CARLI CONSORTIUM on June 29, 2009
Published on February 6, 2001 on http://pubs.acs.org | doi: 10.1021/om000548e

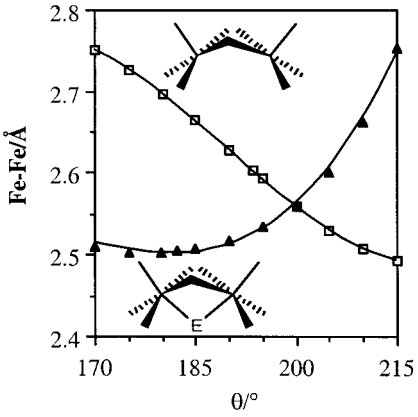

Figure 4. Dependence of the Fe−Fe bond distance on the orientation of the terminal ligands (**2a**) in the $[Fe_2(CO)_8]^{2-}$ anion with structure **1b** (squares) and in the adducts $[Fe_2(\mu\text{-E})(CO)_8]$ with structure **3b** (triangles).

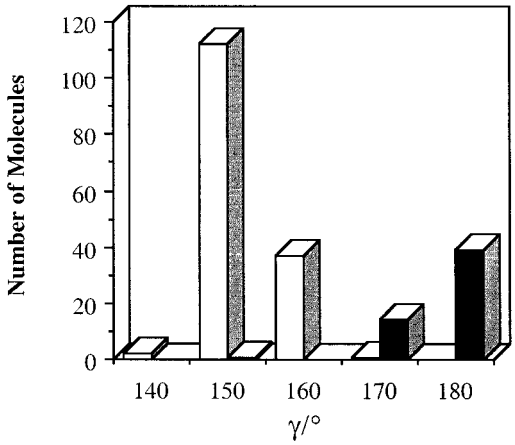

Figure 5. Histogram indicating the distribution of the angle γ defining the orientation of terminal equatorial ligands in adducts of types $[Fe_2(\mu\text{-E})(CO)_8]$ (**3c**, white bars) and $[Fe_2(\mu\text{-E})_2(CO)_8]$ (**3c′**, black bars), as found in the Cambridge Structural Database.

4) and that bond is expected to be little affected for angles of up to 200°. The experimental Fe−Fe distances in several adducts (more than 32 compounds, see Supporting Information) are in excellent agreement with the values predicted for $[Fe_2(CO)_6(\mu\text{-CO})_2(\mu\text{-CH}_2)]$. In summary, shorter Fe−Fe distances are expected for triple-bridged adducts than for the doubly bridged dianion.

Let us now analyze the adducts derived from form **1d** of $[Fe_2(CO)_8]^{2-}$. The dianion can associate an electrophile by simultaneously bonding to the two Fe atoms in a bridging position, as in $[Fe_2(CO)_8(\mu\text{-E})]$, eventually adding a second bridging electrophile to form $[Fe_2(CO)_8(\mu\text{-E})_2]$ (**3c′**). The orientation of the terminal ligands can be defined by the angle between the metal−metal bond and the bisector of the two $Fe-C_{eq}$ bonds, γ in **3c**. Obviously, for compounds with two bridging electrophiles the terminal equatorial carbonyls must remain symmetric as in the parent anion, and γ is expected to be around 180°, in good agreement with the experimental data (Figure 5). Some trends for predicting the stability of the metal−metal interaction in this kind of adducts have been discussed previously by us, based on semiempirical and density functional calculations.[32] In contrast, compounds with one bridging electrophile (**3c**)

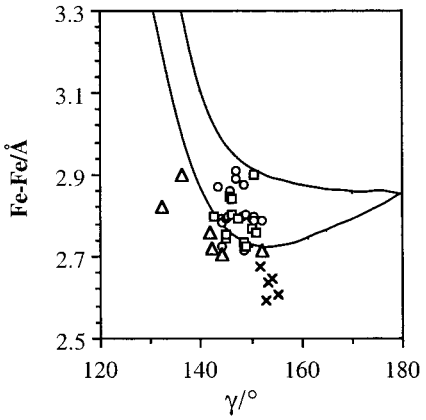

Figure 6. Calculated Fe−Fe distances as a function of γ in $[Fe_2(CO)_8]^{2-}$ (upper line) and $[Fe_2(\mu\text{-CH}_2)(CO)_8]$ (lower line) derived from **1c**. Experimental data for $[Fe_2(\mu\text{-E})(CO)_8]$ adducts with bridging carbon atoms (crosses), other group 14 elements (circles), group 13 or 15 elements (squares), and transition metals (triangles) are also shown for comparison.

are expected to undergo an important ligand rearrangement from its parent structure **1c**. According to our calculations on the model compound $[Fe_2(CO)_8(\mu\text{-CH}_2)]$, the optimum geometry has $\gamma \approx 161°$ and the corresponding distortion in the parent dianion costs barely 2.1 kcal/mol. Our calculations on the same model complex predict that the orientation of the equatorial ligands affects the metal−metal bond length (Figure 6) in the $[Fe_2(CO)_8(\mu\text{-CH}_2)]$ complex, with the shortest distances found at around $\gamma = 150°$. The experimental range of γ for such compounds is 150−160°, in fair agreement with the theoretical predictions (Figure 6), although a clear correlation between γ and Fe−Fe cannot be appreciated due to the diversity of the structurally characterized compounds. Only for the family of trinuclear clusters (i.e., the adducts in which E is a transition metal fragment) does one find two structures with significantly smaller angles and correspondingly larger Fe−Fe distances as predicted by our calculations.

Two electrophiles can alternatively be linked in terminal positions to one Fe atom each as in $[Fe_2(CO)_8E_2]$ (**3a**), a system studied earlier with a semiempirical MO method.[30] According to our present calculations, the **1a** dianion needs about 8 kcal/mol to adopt the configuration found in the $[Fe_2(CO)_8E_2]$ adduct **3a**, for which a significant rearrangement of the equatorial carbonyl ligands is needed. A correlation is found between the pyramidality angle α (i.e., the average of the Fe−Fe−C bond angles involving equatorial ligands) and the Fe−Fe bond distance. For the model compound $[Fe_2(CO)_8Me_2]$, we have optimized the structure at different pyramidality angles (Figure 7, squares), and a parabolic dependence of the Fe−Fe distance on α is found. Since the region of minimum energy corresponds to the left branch of the parabola, the Fe−Fe bond distance is predicted to decrease upon increasing α. We have previously found a similar behavior for other metal−metal bonds.[33] Although the number of available experimental data are scarce, the trend is evident

(32) Palacios, A. A.; Aullón, G.; Alemany, P.; Alvarez, S. *Inorg. Chem.* **2000**, *39*, 3166.
(33) Liu, X.-Y.; Alvarez, S. *Inorg. Chem.* **1997**, *36*, 1055.

Downloaded by CARLI CONSORTIUM on June 29, 2009
Published on February 6, 2001 on http://pubs.acs.org | doi: 10.1021/om000548e

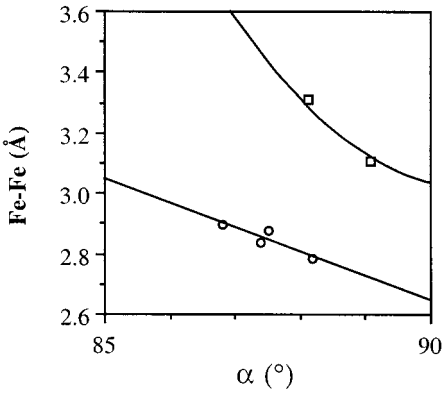

Figure 7. Calculated Fe−Fe bond distance as a function of the pyramidality α for $[Fe_2Me_2(CO)_8]$ in the **3a** structure (squares, only the left branch of the parabola shown). Experimental data for $[Fe_2E_2(CO)_8]$ complexes are also shown (circles).

(Figure 7), even if at shorter distances than calculated. The least-squares fitting of the calculated data gives eq 2.

$$d = 2.648 + 4.577 \cos \alpha \qquad (2)$$

The susceptibility to pyramidalization for this family of complexes, given by the slope of eq 2, is larger than previously found for other transition metals with varying metal−metal bond orders, although the established trends already suggested that the largest susceptibility should appear for single bonds between first-row transition metals.[34] The intrinsic Fe−Fe bond distance (that at $\alpha = 90°$, given by the intercept in eq 2) is practically identical to the longest one found so far, corresponding to Ru^I−Ru^I single bonds.[34]

The last type of adduct we consider is **3e**, with two electrophiles in terminal positions, which can be derived from structures **1e** or **1f** of the binuclear carbonylate. Preparing the $[Fe_2(CO)_8]^{2-}$ anion for bonding in this structure is strongly destabilizing (more than 34 kcal/mol above the most stable form **1c**, see Scheme 1), a fact that suggests a high activation energy for the formation of such Fe adducts from the dianion. Although no Fe derivatives with this structure have been found in a structural database search, the structures of a few Ru and Os compounds have been reported (see Supporting Information). Consistently, a look at the synthetic literature indicates that all compounds with structure **3e** are actually prepared from the unbridged trinuclear clusters $[M_3(CO)_{12}]$, a starting product that is not available for M = Fe.

Conclusions

In the present theoretical study we have analyzed twelve different structures for the $[Fe_2(CO)_8]^{2-}$ anion and found nine stationary points in its potential energy surface. Three of these points are true minima corresponding to geometries **1a**−**c** and show energy differences of less than 3 kcal/mol. Two low-energy transition states (**TS1** and **TS2**) connecting these minima have also been characterized, as well as two transition states at higher energies corresponding to rotations around the Fe−Fe bond (**1d** and **1g**). These results are consistent with the **1a** structure found for all salts of $[Fe_2(CO)_8]^{2-}$ in the solid state and with the isomerization reactions detected in solution. The Fe−Fe bond distance is highly sensitive to the arrangement of the ligands. As a rule of thumb, we can conclude that (a) shorter distances appear when the two Fe atoms are in a square pyramidal arrangement; (b) for trigonal bipyramidal coordination, the staggered rotamers present shorter distances than the eclipsed ones; and (c) equatorial Fe−Fe bonds are shorter than axial ones, other things being equal. No correlation exists between the optimized Fe−Fe bond distances and the calculated energy for each isomer.

The orientation of the terminal carbonyl ligands in the bridged isomer **1b**, calibrated by the angle θ, is expected to affect the Fe−Fe bond distance. This effect is not appreciated in the known structures of several salts of $[Fe_2(CO)_8]^{2-}$, all with similar values of θ, but can be found in isoelectronic cobalt complexes. Rotation of the two monomeric units around the Fe−Fe bond presents substantial barriers of 9.6 (for **1a**) and 16.7 (**1c**) kcal/mol. The distorted structure **1h** that is found in $[MRu(CO)_8]^{2-}$ (M = Fe, Ru) is not a minimum for $[Fe_2(CO)_8]^{2-}$, although it is found to be only 2.2 kcal/mol higher than the most stable structure **1c**.

The analysis of the Fe−Fe stretching region of the calculated vibrational spectra allowed us to find an excellent correlation between the Fe−Fe distance and $\ln(k_{FeFe})$, where k_{FeFe} is the stretching force constant. This correlation is consistent with that reported previously by Harvey for experimental data, but extends the range of applicability to much longer bond distances. In the CO stretching region, two bands are expected for **1b** at frequencies characteristic of bridging carbonyls (1680−1700 cm^{-1}), together with three strong bands between 1800 and 1900 cm^{-1} in the infrared spectrum. Isomers **1a** and **1c** are predicted to present very similar infrared spectra, with two intense bands between 1830 and 1850 cm^{-1}.

The reorganization of the terminal carbonyl ligands (from $\theta = 194°$ to $\theta = 182°$) required to bond an electrophile in a bridging position, as in **3b**, costs only 2 kcal/mol. The doubly bridged adducts of type **3c** can be obtained from the **1d** structure, which is 16.7 kcal/mol higher than the most stable form of $[Fe_2(CO)_8]^{2-}$, with no significant reorientation of the terminal ligands. In contrast, structure of type **3a** requires 8 kcal/mol for ligand reorientation and is expected to appear only when the bidentate nature of the electrophile makes the alternative structures unattainable. Adducts with two terminal electrophiles of type **3e** could be obtained from structures **1e** or **1f** of the dianion, but these are high-energy forms and this synthetic route seems to be unpractical. If these compounds could be made, a strong pyramidality effect should be expected for the Fe−Fe bond, with the largest susceptibility to pyramidalization known so far, together with a quite long intrinsic Fe−

(34) Aullón, G.; Alvarez, S. *J. Chem. Soc., Dalton Trans.* **1997**, 2681.

(35) Frisch, M. J.; Trucks, G. W.; Schlegel, H. B.; Gill, P. M. W.; Johnson, B. G.; Robb, M. A.; Cheeseman, J. R.; Keith, T. A.; Petersson, G. A.; Montgomery, J. A.; Raghavachari, K.; Al-Laham, M. A.; Zakrzewski, V. G.; Ortiz, J. V.; Foresman, J. B.; Cioslowski, J.; Stefanov, B. B.; Nanayakkara, A.; Challacombe, M.; Peng, C. Y.; Ayala, P. Y.; Chen, W.; Wong, M. W.; Andrés, J. L.; Replogle, E. S.; Gomperts, R.; Martin, R. L.; Fox, D. J.; Binkley, J. S.; Defrees, D. J.; Baker, J. P.; Stewart, J. P.; Head-Gordon, M.; Gonzalez, C.; Pople, J. A. *Gaussian 94 (Revision E.1)*; Gaussian Inc.: Pittsburgh, PA, 1995.

Downloaded by CARLI CONSORTIUM on June 29, 2009
Published on February 6, 2001 on http://pubs.acs.org | doi: 10.1021/om000548e

Fe bond length. Such a pyramidality effect is actually found in compounds with structure **3a**, both computationally and in the experimental structural data.

Computational Details

Density functional calculations were carried out using the GAUSSIAN94 package.[35] The hybrid B3LYP-DFT method was applied, in which the Becke three-parameter exchange functional[36] and the Lee−Yang−Parr correlation functional[37] were used. The double-ζ basis set for the valence and outermost core orbitals combined with pseudopotentials known as LANL2DZ were used for all the atoms.[38,39] The geometries were fully optimized using gradient techniques. The zero-point energies of the three minima and transition states **TS1** and **TS2** were also calculated, but the relative energies change by less than 0.3 kcal/mol.

Since the coordination sphere of the iron atoms in the carbonylate dianion $[Fe_2(CO)_8]^{2-}$ is similar to that in the parent complex, $[Fe(CO)_5]$, test calculations were carried out for the latter as a verification of the accuracy of the present calculations, and the main results, together with experimental data and results from previous theoretical studies, are provided as Supporting Information. The present level of computation gives calculated bond distances within 0.012 Å of the experimental data for the trigonal bipyramidal structure of $[Fe(CO)_5]$ and in agreement with other computational works, including multireference CI calculations. Also the energy difference between the square pyramidal and trigonal bipyramidal structures (2.0 kcal/mol higher for the former) is in excellent agreement with other calculations and with experimental estimates obtained from ^{13}C NMR spectral data.

(36) Becke, A. D. *J. Chem. Phys.* **1993**, *98*, 5648.
(37) Lee, C.; Yang, W.; Parr, R. G. *Phys. Rev., B* **1988**, *37*, 785.
(38) Dunning, T. H., Jr.; Hay, P. J. *Modern Theoretical Chemistry*; Plenum: New York, 1976; p 1.
(39) Hay, P. J.; Wadt, W. R. *J. Chem. Phys.* **1985**, *82*, 299.

Structural Analysis. Collection of structural data was retrieved from the Cambridge Structural Database (Version 5.18, October 1999).[31] Our search included compounds with several cores having two group 8 metal atoms and eight carbonyl ligands.

Acknowledgment. Financial support for this work was provided by the Dirección General de Enseñanza Superior (DGES) through Grant PB98-1166-C02-01 and by Comissionat per a Universitats i Recerca (Generalitat de Catalunya) through Grant SGR99-0046. The computing resources at the Centre de Supercomputació de Catalunya (CESCA) were made available in part through grants from Comissió Interdepartamental per a la Recerca i la Innovació Tecnològica (CIRIT) and from the Universitat de Barcelona. The authors are indebted to A. Solé and S. Olivella for discussions and advice, and to O. Rossell for a critical reading of the manuscript.

Supporting Information Available: The following data are supplied as Supporting Information: (i) calculated vibrational data in the $\bar{\nu}$(CO) region (Table S1) and corresponding experimental data (Table S2); (ii) CSD frequencies of structures **3b**−**3e** for adducts of the type $[E_nM_2(CO)_8]$, where M = Fe, Ru, Os; E = metal atom of periodic groups 13−15, d^{10}-ML, d^{12}-ML_2, or d^8-ML_4 transition metal fragments (Table S3); (iii) Fe−Fe distances and orientation angles of the $Fe(CO)_3$ groups (θ) in experimental (Table S4) and calculated (Table S5) structures of type **3b** for complexes $[Fe_2(CO)_6(\mu\text{-}CO)_2(\mu\text{-}E)]$; (iv) experimental structural data and CSD refcodes for compounds with **3e** structure (Table S6), and (v) atomic coordinates for the two geometries of $[Fe(CO)_5]$ (Table S7), for the three minimum energy structures of $[Fe_2(CO)_8]^{2-}$ (**1a**−**1c**) and for the transition states **TS1**, **TS2**, **1d**, and **1g** (Tables S8). This material is available free of charge via the Internet at http://pubs.acs.org.

OM000548E

Downloaded by CARLI CONSORTIUM on June 29, 2009
Published on February 6, 2001 on http://pubs.acs.org | doi: 10.1021/om000548e